# Engineering the plasmonic optical properties of cubic silver nanostructures based on Fano resonance

Zhi Yang, Minqiang Wang, Xiaohui Song, Jianping Deng, and Xi Yao

Citation: J. Chem. Phys. **139**, 164713 (2013); doi: 10.1063/1.4826626
View online: http://dx.doi.org/10.1063/1.4826626
View Table of Contents: http://jcp.aip.org/resource/1/JCPSA6/v139/i16
Published by the AIP Publishing LLC.

# Engineering the plasmonic optical properties of cubic silver nanostructures based on Fano resonance

Zhi Yang (杨智), Minqiang Wang (汪敏强),[a] Xiaohui Song (宋孝辉), Jianping Deng (邓建平), and Xi Yao (姚熹)
*Electronic Materials Research Laboratory (EMRL), Key Laboratory of Education Ministry, International Center for Dielectric Research, Xi'an Jiaotong University, Xi'an 710049, China*

(Received 20 June 2013; accepted 3 October 2013; published online 30 October 2013)

The plasmonic optical properties of nanostructures including a dimer, a linear chain, a T-shaped nanostructure, and a 2D array consisting of Ag nanocubes have been investigated using the discrete dipole approximation method. The simulation results indicate that both the interparticle gap and polarization have an important impact on far-field and near-field characteristics. With decreasing interparticle distance for four nanostructures, the plasmon resonance peak is monotonically red-shifted and the electric intensity enhancement factor increases rapidly due to increased interparticle coupling interaction. Moreover, we also find that a T-shaped nanostructure has the largest electric intensity enhancement factor compared with other three nanostructures due to the coupling interaction at the intersection. This coupling is caused by the radiative interference between subradiant and superradiant resulting in Fano resonance. These results show how nanostructure arrangement design, gap adjustment, and polarization control can be used to achieve high field enhancements.
 [http://dx.doi.org/10.1063/1.4826626]

## I. INTRODUCTION

For several decades, the noble metal nanoparticles have attracted huge interest because of their excellent adjustable plasmonic optical properties by tailoring the size, shape, and environment. Among all noble metal materials, there is a large number of studies on Ag nanoparticles due to its strongest localized surface plasmon resonance (LSPR) and broad resonance spectral range across from 300 to 1200 nm.[1] The LSPR arises when the oscillating electric field of the incident light resonantly couples to the conduction electrons making them collectively oscillate at the certain frequency.[2] So far, there is a lot of research both experimental and theoretical about the plasmonic properties of metal nanoparticles with different shapes (sphere, cube, rod, and triangle plate).[3,4]

Furthermore, the nanostructures assembled by Ag nanoparticles from 1D to 2D have many novel plasmonic features due to surface plasmon coupling. These nanostructures include a dimer, a linear chain, a T-shaped nanostructure, and a 2D array. Among these, a dimer can be the simplest assembled nanostructure. Previously, Schatz *et al.* have investigated electromagnetic fields around Ag dimers of sphere and triangular prisms in detail.[5] Recently, Schatz *et al.* have reported the synthesis of solution-dispersible gold nanorod dimers with gaps as small as 2 nm for surface-enhanced Raman scattering (SERS).[6] Xia's group have prepared Ag nanocubes dimer based on plasma etching, and measured SERS enhancement factor depending on incident polarization.[7] Kim *et al.* carried out the near-field optical mapping of gold nanocubes dimers to directly investigate the strong coupling between two adjacent nanocubes.[8] Grillet *et al.* measured absolute extinction cross section of individual Ag nanocube dimers using spatial modulation spectroscopy technique, and their results were supported by discrete dipole approximation calculations.[9] Extending a dimer to a linear chain can produce huge difference in both far-field and near-field, and a linear chain can be used to transport electromagnetic energy like waveguide. Zhang's group have studied experimentally and theoretically that the plasmon resonance wavelength was significantly red-shifted with the increased nanoparticle number in 1D chain.[10] Moreover, Maier *et al.* observed that plasmon shift saturated and the infinite chain limit was typically reached for chains consisting of about ten nanoparticles because near-field interactions could be negligible for larger separations.[11] So we chose linear chains consisting of ten nanocubes in this study. Another experimental study was conducted by Nomura *et al.*, who have measured a plasmon propagation length of 4 $\mu$m for a chain of 230 nm gold nanoparticles with gaps of 70 nm.[12] Recently, Gao *et al* reported that polymer-grafted Ag nanocubes could be self-assembled into 1D chain that had well-defined interparticle orientations in experiment.[13] Furthermore, they investigated different plasmonic response of edge–edge-oriented nanocubes and face–face-oriented nanocubes with different oriented nanojunctions. All the works mentioned above can greatly support this study.

Besides, a T-shaped nanostructure attracts people's interest because it can bend light around corners or split light into two branches, which can be used to direct energy transfer. In particular, Seideman's group firstly reported that the phase and polarization of the excitation source could be introduced as tools to control over the pathway of light at the intersection of a T-shaped nanostructure,[14,15] which provided a new way to transfer electromagnetic energy in plasmonic

[a]Author to whom correspondence should be addressed. Electronic mail: mqwang@mail.xjtu.edu.cn. Tel.: +86-29-82668794.

 

nanodevices. Finally, 2D periodically arranged nanocubes can be a plasmonic crystal. Maier *et al.* have used this system to study Fano resonance because of its ability to exhibit very sharp and strong spectrum.[16] Besides, the 2D nanostructure array can be well-ordered and close-packed metal nanoparticles superlattices, which can be prepared by chemical method including controlled evaporation of the solvent and Langmuir-Blodgett techniques.[17] Chen *et al.* observed a red shift at the plasmon resonance wavelength with decreasing interparticle distance in experiment.[18] These studies mentioned above mainly focus on the property of individual nanostructure, so it is hard to find the impact of nanostructure arrangement on field distribution and enhancement under the same situation. To our knowledge, there are few reports that have a detailed comparison of four nanostructures from 1D to 2D.

In this paper, we report that the optical properties of four nanostructures consisting of Ag nanocubes can be adjusted by interparticle gap and incidence polarization. By comparing four nanostructures, we can find the dependence of field distribution and enhancement on nanostructure arrangement. Moreover, we assign different plasmon resonance modes based on surface charge distribution and some references. Combining the plasmon hybridization theory, we can show how the plasmon coupling interaction naturally determines the plasmon resonance modes which cause the change of far-field and near-field characteristic. In particular, we explain why there is the largest field enhancement for a T-shaped nanostructure based on Fano resonance.

## II. NUMERICAL CALCULATION METHOD

To simulate the far-field optical characteristic and near-field mapping of plasmon around complex metal nanostructures, a flexible and general numerical tool based on electrodynamic theory is needed. Over the past years, many numerical methods have been introduced, including discrete dipole approximation (DDA) method, the finite difference time domain (FDTD) method, and the finite element method (FEM).[19] Among these methods, the DDA theory was developed by Purcell and Pennypacker.[20] After some improvements, Draine and Flatau implemented this theory in DDSCAT program, which allowed that this method could be used to calculate scattering, absorption of targets with arbitrary geometries, and complex refractive index. In particular, our works benefited from efficient near-field calculations implemented recently,[21] which enabled us to use this powerful tool to solve the plasmonic problem of complex metal nanostructures. In the DDA method, the continuum target is represented as a cubic array of N polarizable elements. The electromagnetic scattering problem that an incident periodic wave interacts with this array of point dipoles is then solved self-consistently. In order to minimize the errors, the interdipole spacing $d$ should be small enough compared with the distinctive structural feature of the target. For an accurate calculation, $|m|kd < 0.5$ should be met,[22] where $m$ is the complex refractive index of the target material; $k = 2\pi/\lambda$, where $\lambda$ is the wavelength *in vacuo*; and $d$ is the interdipole spacing.

For our calculation, the latest available DDSCAT 7.2 program was used here. In order to describe conveniently, we defined the axis connecting nanoparticles as long axis, and the axis perpendicular to long axis in xoz plane as short axis for four nanostructures. Besides, we defined Lab Frame in which the incident radiation propagated in the +x direction, and linearly polarized along the z direction. The Target Frame was defined by setting target axis $a_1$ as (1, 0, 0). The incident angle $\alpha$ was specified by incident direction and target axis $a_1$. Every Ag nanocube with side length of 5 nm was represented by 1000 dipoles, so the interdipole space was 0.5 nm, which was small enough to minimize the errors. Such a fine discrete dipole approximation of the single Ag nanocube was checked to achieve both a quite good shape definition and a proper convergence of the calculations. Therefore, we always kept the same interdipole spacing whatever the number of nanoparticles and the interparticle separated distance were. The effective radius $a_{eff}$ of Ag nanocube, that was, the radius of a sphere of equal volume, was needed in calculation. It was 3.9 nm, 6.7 nm, 7.3 nm, and 14.4 nm for a dimer, a linear chain, a T-shaped nanostructure, and a 2D array, respectively. The refractive index of ambient dielectric was 1.46. This value was chosen because it corresponded to the refractive index of oleic acid which was often used in the case of Ag nanoparticles synthesis.[23] Besides, the surface charge distribution profile of nanostructure was calculated by FEM to assign the resonance mode correctly.

When the sizes of novel metal nanoparticles are less than several tens of nanometers, the conduction electrons suffer an additional damping process due to their scattering from the nanoparticle surface, resulting in a reduced effective mean free path. Therefore, the size correction of dielectric function becomes necessary.[24] The dielectric function of Ag nanocubes was calculated by size correction in Eq. (1):[25]

$$\varepsilon(\omega, L_{eff}) = \varepsilon_b(\omega) + \frac{\omega_p^2}{\omega(\omega + i\omega\gamma_0)} - \frac{\omega_p^2}{\omega(\omega + i\omega\gamma_0 + i\omega v_F/a_{eff})}, \quad (1)$$

where $\varepsilon_b$ was the bulk dielectric function from experimental values of Johnson and Christy,[26] $\omega_p$ was the plasma angular frequency of 9.6 eV, $\gamma_0$ was the damping constant of 0.018 eV, $v_F$ was the Fermi velocity of $1.4 \times 10^6$ m/s,[24] and $a_{eff}$ was the effective particle radius.

## III. RESULTS AND DISCUSSION

### A. Far-field optical characteristic

Seen from Figure 1, there always exist six resonance peaks regardless of the number of nanocubes for four nanostructures. Recently, Near *et al.* had a detailed investigation on the relationship between extinction peak and plasmon resonance mode in the extinction spectrum of Ag nanocube using DDA method.[27] The plasmon resonance modes at the different extinction peaks were assigned correctly by plotting field vector orientations around nanoparticles. The results indicated that it was always dipole mode at the largest plasmon resonance peak (LPRP) whatever the size of nanocube was, while higher-order multipolar plasmon modes appeared at

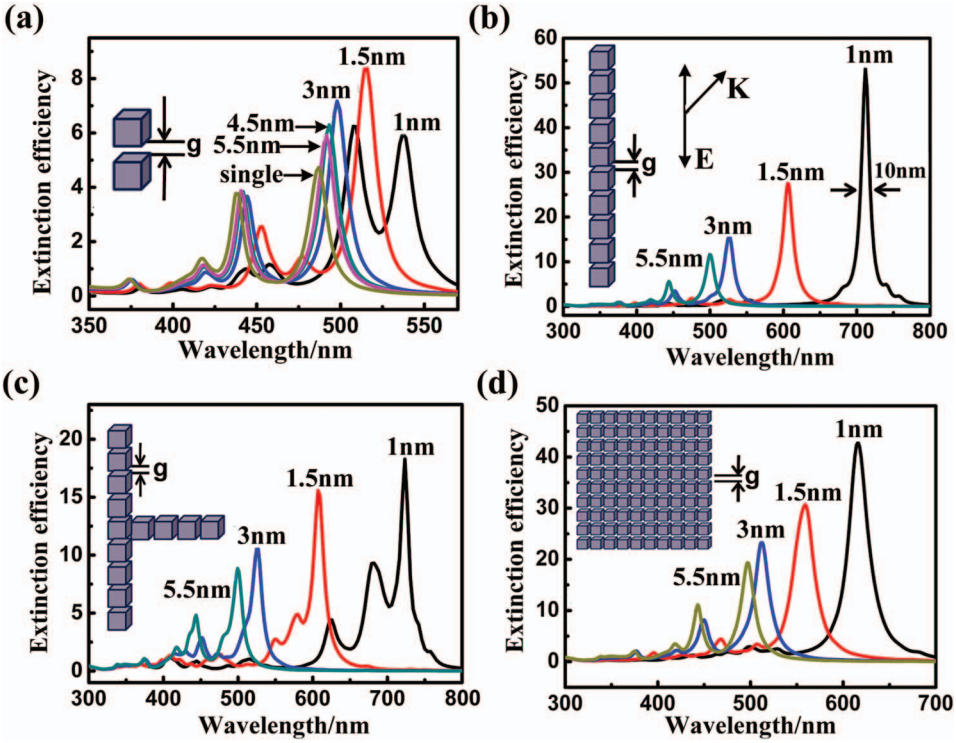


FIG. 1. The extinction efficiency spectrum for (a) a dimer, (b) a linear chain, (c) a T-shaped nanostructure, and (d) a 2D array arranged from Ag nanocubes with different interparticle distances. Inset is the schematic which depicted the geometry of the system. The incidence and polarization directions for four nanostructures are the same.

small extinction peak. Moreover, the LPRP always appeared at the largest resonance wavelength, while small extinction peak appeared at short resonance wavelength. This property is further confirmed by experimental observation. Recently, Mazzucco *et al.* have observed near-field mapping around individual subwavelength-sized silver nanocubes by means of electron energy loss spectroscopy,[28] which indicated the relationship between plasmon resonance mode and certain resonance peak in the extinction spectrum. Next, we will mainly pay attention to the LPRP for four nanostructures because many applications choose wavelength based on the LPRP from the experimentally collected extinction spectrum.

Figure 1 presents the extinction efficiency spectrum of four nanostructures with different interparticle distances at incidence angle of 0°. It indicates that the LPRP is monotonically red-shifted with decreasing nanoparticles separation, and the extinction efficiency reaches its maximum value when the interparticle distance of two Ag nanocubes is 1 nm. This phenomenon can be explained by the capacitive coupling between the plasmon modes of two adjacent Ag nanocubes resulting in hybridized states.[29] Similarity, Grillet *et al* explained the plasmonic coupling between two Ag nanocubes results from the electrostatic interaction between the electron charge distributions induced on both facing surfaces.[9] When the interparticle distance is 5.5 nm, the coupling of two nanocubes is very weak, which makes the extinction spectrum of four nanostructures similar to that of single nanocube. However, when two adjacent Ag nanocubes approach each other to 1 nm, the coupling interaction of plasmon modes in two nanocubes becomes very strong. Moreover, the LPRP is red-shifted to different wavelengths for four nanostructures with the same interparticle distance. A T-shaped nanostructure has the largest red shift to 723 nm while keeping the interparticle distance of 1 nm, which indicates that a T-shaped nanostructure has the strongest coupling interaction. The detailed analysis about impacting of strong coupling on near-field distribution will be provided later in this paper.

A more interesting phenomenon is that the line shapes of extinction spectrum are quite different for four nanostructures. For symmetric nanostructure like a dimer, a linear chain, and a 2D array, the line shapes are always symmetric. However, for asymmetric nanostructure such as a T-shaped nanostructure, the asymmetric line shape appears in Figure 1(c). At the same time, for other asymmetric nanostructures like dolmen structure[16] and split-ring,[30] the asymmetric line shape based on Fano resonance also forms. The Fano resonance is caused by the radiative interference effects, and it can be particularly important for arrays of nanoparticles.[31] Furthermore, the radiative interference can be described clearly by plasmon hybridization modes. The hybridization schematic is shown in Figures 2(a) and 2(c). Combining surface charge distribution profile in Figure 2(b), we can deeply understand how the Fano resonance forms for a T-shaped nanostructure under the coupling interference of different resonance modes. For longitudinal mode in Figure 2(a), collective oscillation of electron clouds is slowed by the electrostatic attraction between high charge densities of opposite sign sustained on the facing surfaces of nanocubes when dipole alignment of two nanocubes is parallel.[9] So we define parallel dipole alignment as bonding mode, which corresponds to low-energy and LPRP; while the opposite dipole alignment causes an antibonding mode, which corresponds

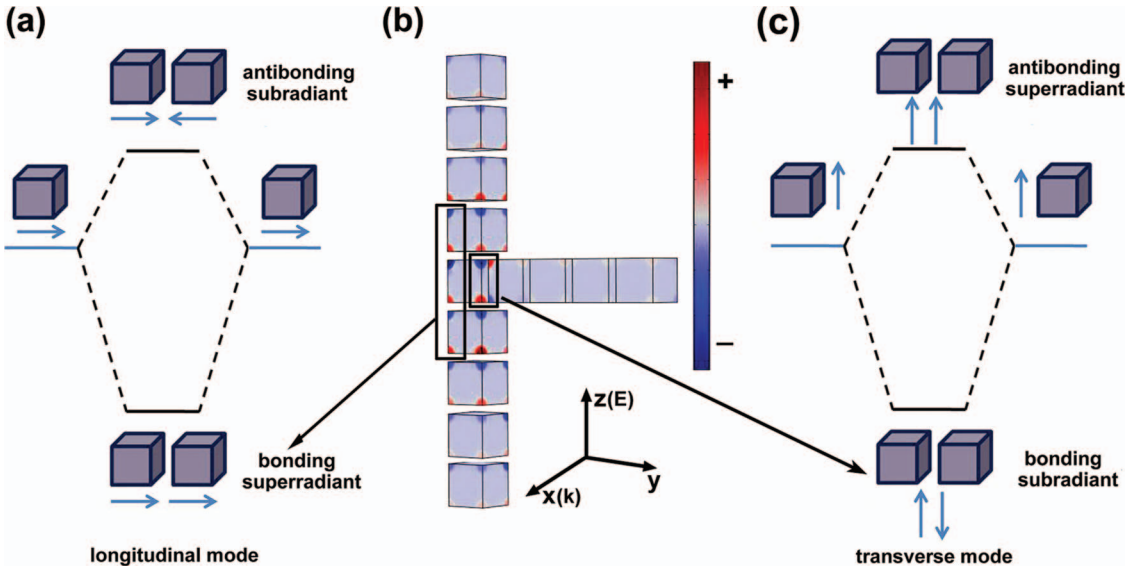


FIG. 2. Schematic illustrating the relationship between the orientation of the dipole moments and plasmon hybridization modes under the longitudinal mode (a) and transverse mode (c). (b) Surface charge distributions of T-shaped nanostructure calculated by FEM at the LPRP position (723 nm).

to high-energy.[32,33] In this situation, the bonding mode has increased total dipole moment, which is superradiant, and the antibonding mode is subradiant.[31,34] While for transverse mode in Figure 2(c), the bonding mode has a reduced total dipole moment, which is subradiant, and the antibonding mode is superradiant. So the Fano resonance is the result of interference between superradiant and subradiant modes. The more detailed discussion will be appeared in near-field mapping of a T-shaped nanostructure. It was noted that Sonnefraud *et al.* explored Fano resonance resulted from interference between subradiant and superradiant modes in concentric ring-disk cavity nanostructure.[35] Compared with our study, the ring-disk nanostructure is radial excitation. So the opposite dipole alignment causes a bonding mode, which is subradiant, while the parallel dipole alignment is antibonding mode, which is superradiant.

Besides, the width of the LPRP gradually decreases and full-width at half-maximum (FWHM) decreases to 10 nm when the interparticle distance is 1 nm. Hicks *et al.* explained this narrowing of the collective plasmon mode induced by far-field diffractive coupling.[36] As a result, it has an important application in surface plasmon resonance sensing since the narrow line width produces improved sensitivity.[31] Moreover, Figure 3 presents the extinction efficiency spectrum of four nanostructures with interparticle distance of 1 nm at different incidence angles. With the incidence angle increasing from 0° to 90°, the incident light polarization is along from the long axis to the short axis. The extinction efficiency of longitudinal plasmon resonance peak decreases monotonically, while that of transverse plasmon resonance peak increases monotonically, and the position of both peaks keeps unchanged, which indicates that the transverse mode is gradually dominated.

### B. Near-field mapping of plasmon

When the incident light linearly polarizes along the long axis, and the interparticle distance is 1 nm, there is the strongest electric intensity for four nanostructures. The cross section of electric intensity is shown in Figure 4. For a dimer, the light is concentrated into exceedingly small volume in the gap between nanoparticles, which creates the huge near-field enhancements. This highly localized, giant electric field enhancement is commonly known as the hot-spot phenomenon.[1] However, there exist different electric field distributions for four nanostructure arrangements. For a linear chain in Figure 4(b), the electric intensity in the central gap area is stronger than that in the both end gap areas. This can be attributed to that the longitudinal plasmon mode supported by a linear chain is no longer localized on the individual nanoparticle but can propagate along the chain axis, which makes it possible to transport electromagnetic energy along the linear chain.[31] Many experimental works can also demonstrate this energy transfer along a linear chain.[37–40] In fact, when interparticle distance decreases to 1 nm, the electric distribution of a linear chain can compare with that of nanorod. As well as, a T-shaped nanostructure can compare with two nanorods arranged in T-shaped configuration, and a 2D array can compare with thin film.

Compared with a linear chain, we can see that the hot-spot is more strongly concentrated in the central gap area of T-shaped nanostructure, and the intersection of two branches has the strongest electric intensity in Figure 4(c). To our knowledge, this unique property has not been reported. We speculate that it may come from the asymmetry of nanostructure. The long branch along the z direction undergoes the longitudinal plasmon mode, while the short branch along the y direction undergoes the transverse plasmon mode. Based on the discussion above, the bonding mode is always dominated for both longitudinal and transverse modes in plasmonic nanostructures due to its low energy. So the longitudinal mode is superradiant, while the transverse mode is subradiant. Furthermore, under the strong coupling condition, the radiative interference between longitudinal and transverse plasmon modes can happen at intersection of this asymmetry nanostructure. It is the interference between

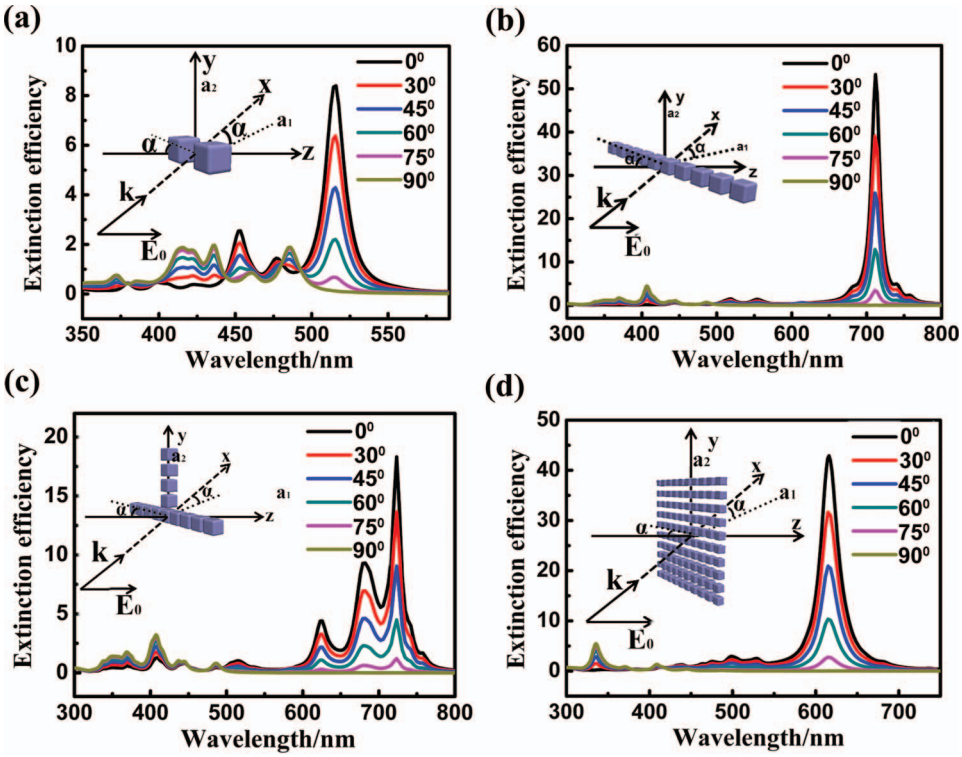


FIG. 3. The dependence of calculated extinction spectra for (a) a dimer, (b) a linear chain, (c) a T-shaped nanostructure, and (d) a 2D array with the same interparticle distances of 1 nm on the incidence angle $\alpha$. Inset is the schematic which depicted the geometry of the system including nanostructure and incident light polarization.

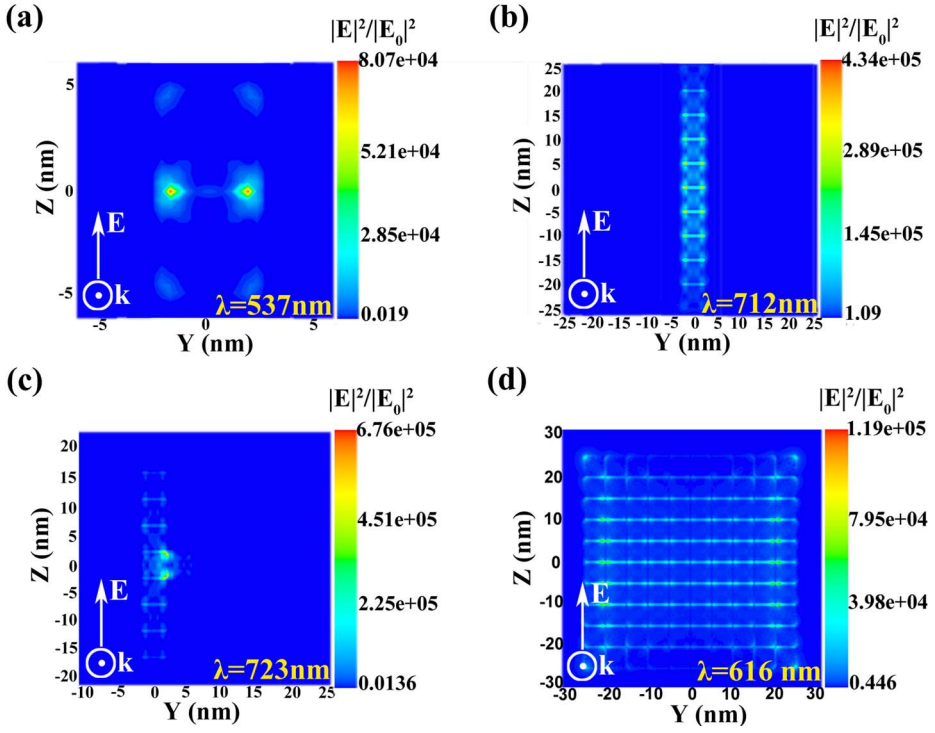


FIG. 4. Electric intensity cross section for four nanostructures with the same interparticle distances of 1 nm at incidence angle of 0°: (a) a dimer, (b) a linear chain, (c) a T-shaped nanostructure, and (d) a 2D array. The wavelength of incident light is shown, which is the strongest extinction peak in plasmon extinction spectrum. The incident light propagated in the +x direction, and linearly polarized along the z direction.

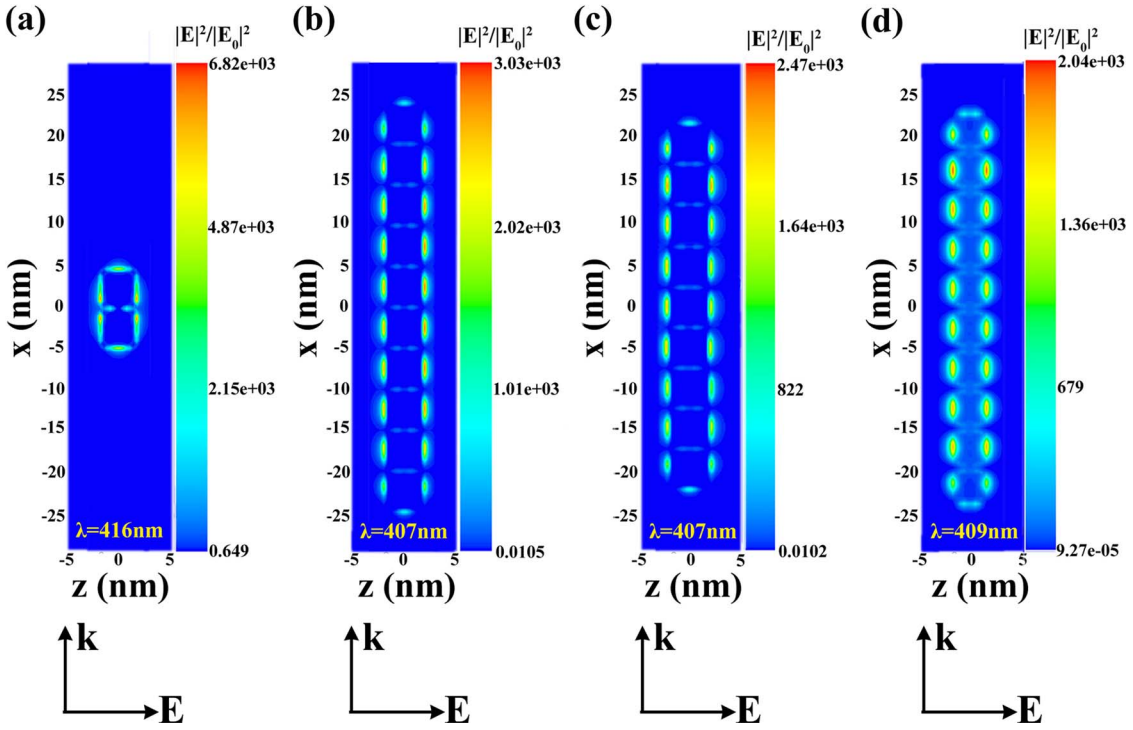


FIG. 5. Electric intensity cross section for four nanostructures with same interparticle distances of 1 nm at incidence angle of 90°: (a) a dimer, (b) a linear chain, (c) a T-shaped nanostructure, and (d) a 2D array. The incident light propagated in the +x direction, and linearly polarized along the z direction. In order to compare transverse modes clearly, the x-z plane from top view was chosen to improve readability.

superradiant and subradiant that produces Fano resonance, which results in bright and dark mode, and asymmetric line shape. Remarkably, Funston's research about two Au nanorods arranged in T-shaped configuration also confirmed this coupling interaction between longitudinal and transverse plasmon modes at intersection by plotting surface charge density profiles.[41] From Figure 2(b), we can see weak surface charge density for transverse plasmon mode along the y direction and strong surface charge density at the intersection. From previous report, it was this intersection that provided an important structure basis for polarization control, which could be used to transfer the electromagnetic energy.[14] The accordance between near-field mapping from DDA method and surface charge density distribution from FEM confirms the above explanation.

For a 2D array in Figure 4(d), the electric intensity is not concentrated into small area like a linear chain and a T-shaped nanostructure even though the interparticle distance keeps small enough to reach strong coupling. So the electric field enhancement for a 2D array is less than that of a linear chain and a T-shaped nanostructure. Unlike the asymmetry of short branch in T-shaped structure, the intersection effect of 2D array with the strong symmetry disappears, and the electric intensity is more equally distributed in 2D array. This near-field mapping is similar to Maier's report about that of the plasmonic crystal, and the Fano resonance has not been produced by this symmetric nanostructure.[16] A 2D array has also been discussed in detail by Schatz,[42] which indicates that radiative damping effects can be negligible for the nanoparticle arrays, and the Fano resonance are evanescent. Besides, the coupled dipole approximation method was also used to calculate the plasmonic properties of Ag nanoparticle array, which get the consistent result with the DDA method.[42,43] Taking different far-field optical characteristics and near-field mappings of four nanostructures, we can know that the electric field enhancement and distribution not only depend on the number of nanocube unit but also have a strong relationship with unit arrangement in nanostructures. Thus, we need to design the arrangement of nanoparticles in nanostructures with predetermined optical properties and functionalities.[44]

Figure 5 compares the different transverse plasmon resonance induced by polarizing along the short axis when the incidence angle keeps 90° for four nanostructures. The incident wavelength is nearly equal for all nanostructures, and the strongest electric intensity locates at the two edges of every cube unit, in accordance with the polarization direction. This indicates that the transverse plasmon resonance is rarely affected by nanostructure because it only happens along the single nanocube unit. So the interparticle dipole coupling interaction can be very weak even though the interparticle distance is small enough.

Here, we define electric intensity enhancement factor as the electric intensity of four nanostructures vs that of single Ag nanocube unit, that is, $|E_{target}|^2/|E_{unit}|^2$. Figure 6(a) shows the dependence of electric intensity enhancement factor on the interparticle distances under the longitudinal plasmon mode. It can be seen that the electric intensity enhancement factor decreases rapidly as the interparticle distances increase for four nanostructures. When interparticle distances are larger than the half of nanocube edge, the electric intensity enhancement factor remains nearly unchanged, which demonstrates that adjusting interparticle gap is an efficient

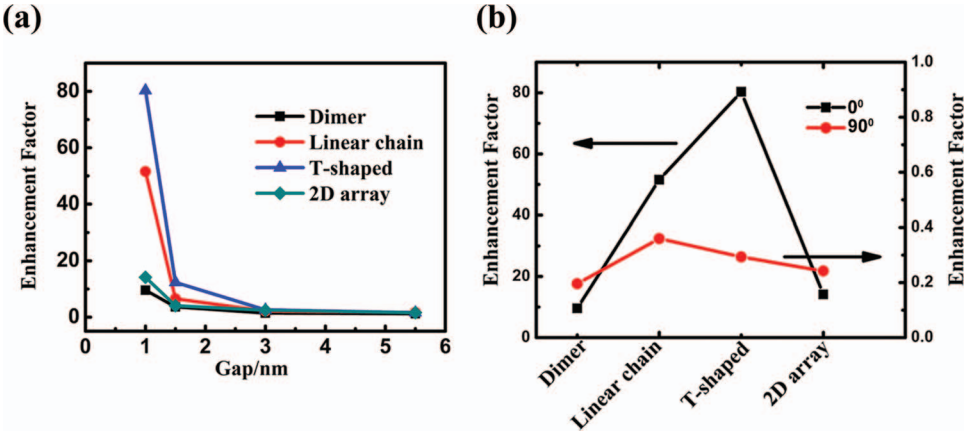


FIG. 6. (a) The dependence of electric intensity enhancement factor for four nanostructures on the interparticle distances at incidence angle of 0°. (b) The comparison of electric intensity enhancement factor for four nanostructures with 1 nm interparticle distance at incidence angle of 0° and 90°, respectively.

way to engineer optical properties of plasmon nanostructures. Besides, a T-shaped nanostructure has the largest electric intensity enhancement factor of 80 compared with other three nanostructures, which indicates that the unit arrangement in nanostructure can also affect the optical properties of plasmon nanostructures. In order to compare the longitudinal and transverse plasmon modes clearly, the corresponding electric intensity enhancement factor of four nanostructures is shown in Figure 6(b). From it, the longitudinal plasmon mode has a larger electric intensity enhancement factor compared with transverse plasmon mode due to stronger interparticle coupling interaction. Therefore, in order to obtain the highest field enhancement for four nanostructures, it is important to control the excitation polarization. Only when the excitation is polarized along the long axis is there a strong plasmon coupling, which produces the associated red shift in LPRP position and large electric field enhancement near the nanostructures.

Even though we have a detailed research on nanostructures from 1D to 2D, when the interparticle separated distance is small enough, the electron transfer between two adjacent cube units may happen. Under this situation, the quantum mechanism effect should be considered.[31] Nordlander *et al.* conducted the full quantum calculation using time-dependent density functional theory (TDDFT) method.[45,46] Recently, Dionne *et al.* analyzed plasmonic properties of particles in the quantum size regime using DFT, and made a direct correlation between a particle's geometry and its plasmon resonance using aberration-corrected transmission electron microscope.[47] Compared with this, our classical calculations overestimate the electric field enhancement near the nanoparticle surface when the interparticle separated distance is small enough. So full quantum calculations are further needed performing to get more accurate electric field enhancement results.

## IV. CONCLUSION

In this paper, we study that the interparticle distances and incident light polarization have great impact on the coupling interaction of plasmon modes in metal nanostructures by DDA simulations, respectively. The calculation results indicate that the electric intensity enhancement factor decreases rapidly as the interparticle distances increase for four nanostructures due to decreased interparticle coupling interaction, and the different incident light polarization produces different plasmon modes. Different far-field optical characteristics and near-field mappings are decided by different unit arrangement in four nanostructures, which results in different applications. The dimer can be widely used in SERS application due to its simple preparation process. The linear chain can be used to transport electromagnetic energy along the linear chain like waveguide. The 2D array has an important application in surface plasmon resonance sensing since its narrow line width produces improved sensitivity. Compared with these nanostructures, a T-shaped nanostructure has the largest electric intensity enhancement factor due to coupling interaction at the intersection, and it provides a new way to transfer electromagnetic energy effectively in plasmonic nanodevices. This indicates that the electric intensity enhancement has a strong relationship with unit arrangement in plasmonic nanostructures. Finally, compared with transverse plasmon mode, the longitudinal plasmon mode has a stronger electric intensity enhancement due to stronger interparticle coupling interaction. The Fano resonance is caused by the radiative interference between subradiant and superradiant in the asymmetric nanostructure like T-shaped nanostructure, not produced in the symmetric 2D nanostructure, because the radiative damping effects can be negligible in symmetric 2D nanostructure.

## ACKNOWLEDGMENTS

The authors gratefully acknowledge financial support from the Natural Science Foundation of China (NSFC) (Grant Nos. 91123019 and 61176056). This work has been financially supported by the International Collaboration Program, the "13115" Innovation Engineering Project of Shaanxi Province (Grant Nos. 2013KW-12-05 and 2010ZDKG-58). We also thank B. T. Draine and P. J. Flatau for using their latest DDSCAT 7.2 version.

[1]M. Rycenga, C. M. Cobley, J. Zeng, W. Li, C. H. Moran, Q. Zhang, D. Qin, and Y. Xia, Chem. Rev. **111**, 3669 (2011).
[2]X. Xu, Z. Yi, X. Li, Y. Wang, X. Geng, J. Luo, B. Luo, Y. Yi, and Y. Tang, J. Phys. Chem. C **116**, 24046 (2012).
[3]B. J. Wiley, S. H. Im, Z.-Y. Li, J. McLellan, A. Siekkinen, and Y. Xia, J. Phys. Chem. B **110**, 15666 (2006).
[4]P. Yang, H. Portales, and M.-P. Pileni, J. Phys. Chem. C **113**, 11597 (2009).
[5]E. Hao and G. C. Schatz, J. Chem. Phys. **120**, 357 (2004).
[6]K. D. Osberg, M. Rycenga, N. Harris, A. L. Schmucker, M. R. Langille, G. C. Schatz, and C. A. Mirkin, Nano Lett. **12**, 3828 (2012).
[7]P. H. C. Camargo, M. Rycenga, L. Au, and Y. Xia, Angew. Chem., Int. Ed. **48**, 2180 (2009).
[8]D.-S. Kim, J. Heo, S.-H. Ahn, S. W. Han, W. S. Yun, and Z. H. Kim, Nano Lett. **9**, 3619 (2009).
[9]N. Grillet, D. Manchon, F. Bertorelle, C. Bonnet, M. Broyer, E. Cottancin, J. Lermé, M. Hillenkamp, and M. Pellarin, ACS Nano **5**, 9450 (2011).
[10]Q. H. Wei, K. H. Su, S. Durant, and X. Zhang, Nano Lett. **4**, 1067 (2004).
[11]S. A. Maier, P. G. Kik, and H. A. Atwater, Appl. Phys. Lett. **81**, 1714 (2002).
[12]W. Nomura, M. Ohtsu, and T. Yatsui, Appl. Phys. Lett. **86**, 181108 (2005).
[13]B. Gao, G. Arya, and A. R. Tao, Nat. Nanotechnol. **7**, 433 (2012).
[14]M. Sukharev and T. Seideman, Nano Lett. **6**, 715 (2006).
[15]M. Sukharev and T. Seideman, J. Chem. Phys. **124**, 144707 (2006).
[16]Y. Francescato, V. Giannini, and S. A. Maier, ACS Nano **6**, 1830 (2012).
[17]Z. Yang, M. Wang, Y. Shi, X. Song, Z. Lin, Z. Ren, and J. Bai, J. Mater. Chem. **22**, 21009 (2012).
[18]C. Chen, S. Tzeng, H. Chen, K. Lin, and S. Gwo, J. Am. Chem. Soc. **130**, 824 (2008).
[19]J. Zhao, A. O. Pinchuk, J. M. McMahon, S. Li, L. K. Ausman, A. L. Atkinson, and G. C. Schatz, Acc. Chem. Res. **41**, 1710 (2008).
[20]B. Draine and P. J. Flatau, J. Opt. Soc. Am. A **11**, 1491 (1994).
[21]P. Flatau and B. Draine, Opt. Express **20**, 1247 (2012).
[22]B. T. Draine and P. J. Flatau, User Guide for the Discrete Dipole Approximation Code DDSCAT 7.2, 2012, see arXiv:1202.3424.
[23]Z. Yang, M. Wang, M. Shi, Y. Shi, and X. Yao, in *Proceedings of the 12th IEEE Conference on Nanotechnology (IEEE-NANO)* (IEEE, 2012), p. 1.
[24]N. Félidj, J. Aubard, and G. Lévi, J. Chem. Phys. **111**, 1195 (1999).
[25]H. Portale`s, N. Pinna, and M. P. Pileni, J. Phys. Chem. A **113**, 4094 (2009).
[26]P. B. Johnson and R. W. Christy, Phys. Rev. B **6**, 4370 (1972).
[27]R. D. Near, S. C. Hayden, and M. A. El-Sayed, J. Phys. Chem. C **116**, 23019 (2012).
[28]S. Mazzucco, N. Geuquet, J. Ye, O. Steéphan, W. Van Roy, P. Van Dorpe, L. Henrard, and M. Kociak, Nano Lett. **12**, 1288 (2012).
[29]P. Nordlander, C. Oubre, E. Prodan, K. Li, and M. Stockman, Nano Lett. **4**, 899 (2004).
[30]N. Liu and H. Giessen, Angew. Chem., Int. Ed. **49**, 9838 (2010).
[31]N. J. Halas, S. Lal, W. S. Chang, S. Link, and P. Nordlander, Chem. Rev. **111**, 3913 (2011).
[32]P. K. Jain, S. Eustis, and M. A. El-Sayed, J. Phys. Chem. B **110**, 18243 (2006).
[33]L. S. Slaughter, Y. Wu, B. A. Willingham, P. Nordlander, and S. Link, ACS Nano **4**, 4657 (2010).
[34]K. Bao, N. A. Mirin, and P. Nordlander, Appl. Phys. A **100**, 333 (2010).
[35]Y. Sonnefraud, N. Verellen, H. Sobhani, G. A. Vandenbosch, V. V. Moshchalkov, P. Van Dorpe, P. Nordlander, and S. A. Maier, ACS Nano **4**, 1664 (2010).
[36]E. M. Hicks, S. Zou, G. C. Schatz, K. G. Spears, R. P. Van Duyne, L. Gunnarsson, T. Rindzevicius, B. Kasemo, and M. Käll, Nano Lett. **5**, 1065 (2005).
[37]T. Shimada, K. Imura, H. Okamoto, and M. Kitajima, Phys. Chem. Chem. Phys. **15**, 4265 (2013).
[38]D. Solis, Jr., B. Willingham, S. L. Nauert, L. S. Slaughter, J. Olson, P. Swanglap, A. Paul, W.-S. Chang, and S. Link, Nano Lett. **12**, 1349 (2012).
[39]S. A. Maier, P. G. Kik, H. A. Atwater, S. Meltzer, E. Harel, B. E. Koel, and A. A. Requicha, Nature Mater. **2**, 229 (2003).
[40]H. Chen, C. He, C. Wang, M. Lin, D. Mitsui, M. Eguchi, T. Teranishi, and S. Gwo, ACS Nano **5**, 8223 (2011).
[41]A. M. Funston, C. Novo, T. J. Davis, and P. Mulvaney, Nano Lett. **9**, 1651 (2009).
[42]C. L. Haynes, A. D. McFarland, L. Zhao, R. P. Van Duyne, G. C. Schatz, L. Gunnarsson, J. Prikulis, B. Kasemo, and M. Käll, J. Phys. Chem. B **107**, 7337 (2003).
[43]S. Yin, Q. Deng, X. Luo, C. Du, and Y. Zhang, J. Appl. Phys. **104**, 024308 (2008).
[44]J. Yelk, M. Sukharev, and T. Seideman, J. Chem. Phys. **129**, 064706 (2008).
[45]J. Zuloaga, E. Prodan, and P. Nordlander, Nano Lett. **9**, 887 (2009).
[46]R. Esteban, A. G. Borisov, P. Nordlander, and J. Aizpurua, Nat. Commun. **3**, 825 (2012).
[47]J. A. Scholl, A. L. Koh, and J. A. Dionne, Nature (London) **483**, 421 (2012).